6-2014

The Human Metapneumovirus Small Hydrophobic Protein has Properties Consistent with Those of a Viroporin and Can Modulate Viral Fusogenic Activity

Cyril Masante
University of Kentucky

Farah El Najjar
University of Kentucky, farah.najjar@uky.edu

Andres Chang
University of Kentucky

Angela Jones
University of Kentucky

Carole L. Moncman
University of Kentucky, carole.moncman@uky.edu

See next page for additional authors

JVI Journals.ASM.org

The Human Metapneumovirus Small Hydrophobic Protein Has Properties Consistent with Those of a Viroporin and Can Modulate Viral Fusogenic Activity

Cyril Masante,* Farah El Najjar, Andres Chang, Angela Jones,* Carole L. Moncman, Rebecca Ellis Dutch

Department of Molecular and Cellular Biochemistry, University of Kentucky, Lexington, Kentucky, USA

ABSTRACT

Human metapneumovirus (HMPV) encodes three glycoproteins: the glycoprotein, which plays a role in glycosaminoglycan binding, the fusion (F) protein, which is necessary and sufficient for both viral binding to the target cell and fusion between the cellular plasma membrane and the viral membrane, and the small hydrophobic (SH) protein, whose function is unclear. The SH protein of the closely related respiratory syncytial virus has been suggested to function as a viroporin, as it forms oligomeric structures consistent with a pore and alters membrane permeability. Our analysis indicates that both the full-length HMPV SH protein and the isolated SH protein transmembrane domain can associate into higher-order oligomers. In addition, HMPV SH expression resulted in increases in permeability to hygromycin B and alteration of subcellular localization of a fluorescent dye, indicating that SH affects membrane permeability. These results suggest that the HMPV SH protein has several characteristics consistent with a putative viroporin. Interestingly, we also report that expression of the HMPV SH protein can significantly decrease HMPV F protein-promoted membrane fusion activity, with the SH extracellular domain and transmembrane domain playing a key role in this inhibition. These results suggest that the HMPV SH protein could regulate both membrane permeability and fusion protein function during viral infection.

IMPORTANCE

Human metapneumovirus (HMPV), first identified in 2001, is a causative agent of severe respiratory tract disease worldwide. The small hydrophobic (SH) protein is one of three glycoproteins encoded by all strains of HMPV, but the function of the HMPV SH protein is unknown. We have determined that the HMPV SH protein can alter the permeability of cellular membranes, suggesting that HMPV SH is a member of a class of proteins termed viroporins, which modulate membrane permeability to facilitate critical steps in a viral life cycle. We also demonstrated that HMPV SH can inhibit the membrane fusion function of the HMPV fusion protein. This work suggests that the HMPV SH protein has several functions, though the steps in the HMPV life cycle impacted by these functions remain to be clarified.

Human metapneumovirus (HMPV) is an enveloped virus belonging to the *Pneumovirinae* genus of the *Paramyxoviridae* family. HMPV is associated worldwide with severe respiratory disease, including bronchiolitis and pneumonia (1). Respiratory tract infections caused by HMPV are an important cause of hospitalizations for children under the age of five, with an annual rate of hospitalization similar to that of influenza (2). HMPV is also an important cause of severe respiratory illness in the elderly (3, 4). Studies indicate that the majority of individuals over the age of five are seropositive for HMPV (1, 5). HMPV was identified in 2001 from samples of patients with respiratory syncytial virus (RSV)-like symptoms, as symptoms of HMPV closely resemble those of RSV (5).

HMPV, like other paramyxoviruses, encodes two surface glycoproteins involved in attachment and entry: the putative attachment protein, termed G for glycoprotein, and the fusion protein, F, which promotes fusion between the cellular and the viral membranes. HMPV is unique among paramyxoviridae, as the F protein is the primary factor for viral attachment in addition to its role in membrane fusion (6, 7). Interestingly, a subset of paramyxoviruses, including members of the pneumoviruses and rubulaviruses and the unclassified J virus, encode an additional surface glycoprotein, termed SH for small hydrophobic protein. The SH protein of most paramyxoviruses is dispensable for viral replication *in vitro* (8–11), though deletion of the avian metapneumovirus (AMPV) SH protein significantly reduced viral replication in cell culture and led to increased syncytium formation (12). Deletion of the SH protein gene affects replication and pathogenicity of a number of paramyxoviruses, including RSV and AMPV, in animal model systems (12–14). Studies suggest that some paramyxovirus SH proteins inhibit apoptosis via a blockade of the tumor necrosis factor alpha (TNF-α)-mediated apoptotic signaling pathway (15, 16).

HMPV SH, a type II integral transmembrane glycoprotein, is the largest SH protein of the viral family (179 amino acids [aa] compared to 65 aa for RSV SH or 175 aa for AMPV SH). Similarly to the RSV SH protein, which exhibits at least four different forms

Received 27 September 2013 **Accepted** 20 March 2014

Published ahead of print 26 March 2014

Editor: D. S. Lyles

Address correspondence to Rebecca Ellis Dutch, rdutc2@uky.edu.

* Present address: Cyril Masante, CNRS UMR 5234, University of Bordeaux, Laboratoire MFP, Bordeaux, France; Angela Jones, Minnesota Department of Health-Public Health Laboratory, St. Paul, Minnesota, USA.

doi:10.1128/JVI.02848-13

depending upon glycosylation level (17), HMPV SH exists in at least three differentially glycosylated forms: unglycosylated (23 kDa), *N*-glycosylated (25 to 30 kDa), and highly glycosylated (80 to 220 kDa) (7). A recombinant HMPV lacking the SH gene was found to replicate in both hamster and nonhuman primate models only marginally less efficiently than wild-type (WT) HMPV (7, 18), indicating that this gene is dispensable in these systems. However, all clinical isolates to date contain an intact SH gene (19, 20), suggesting that HMPV SH plays a functional role during infection. HMPV SH has been suggested to inhibit NF-κB transcriptional activity in airway epithelial cells (21), potentially contributing to pathogenicity of the virus, though a recent study did not support a role for HMPV SH in virus replication or host gene expression (22).

Some paramyxovirus SH proteins have been suggested to be viral protein channels or viroporins. Viroporins are generally small, hydrophobic proteins with one or more transmembrane domains (TMD) which oligomerize to form channels, thereby modifying membrane permeability to ions or small molecules (23). The RSV SH protein is able to alter membrane permeability in bacteria (24) and functions as a cation-selective ion channel in artificial membranes (25), and recent work indicates it has low-pH-activated ion channel activity (26). Fitting with other viroporins, RSV SH can oligomerize as a pentamer (25, 27, 28) and/or a hexamer (29).

To clarify the potential role of HMPV SH, we examined SH oligomerization state, cellular expression and localization, and the effect of SH expression on the synthesis and function of the viral glycoproteins. HMPV SH forms higher-order oligomers, and studies using sedimentation equilibrium analysis demonstrate that the SH protein TMD is sufficient for oligomerization. Similar to other reported viroporins (30, 31), HMPV SH expression increased cell permeability to hygromycin B. HMPV SH expression also significantly altered intracellular localization of a fluorescent dye, suggesting that SH also impacts permeability of intracellular membranes. In addition, HMPV SH expression, while not altering viral glycoprotein trafficking, negatively impacted fusion mediated by the HMPV F protein and to a lesser extent other paramyxovirus fusion proteins. These results suggest that the HMPV SH protein has properties associated with viroporin-like activity.

MATERIALS AND METHODS

Cell lines and virus propagation. Vero, BHK, COS-7, and BSR cells (provided by Karl-Klaus Conzelmann, Max Pettenkofer Institut) were grown in Dulbecco's modified Eagle's medium (DMEM; Gibco Invitrogen, Carlsbad, CA) supplemented with 10% fetal bovine serum (FBS) and 1% penicillin and streptomycin. The medium of BSR cells was supplemented with 0.5 mg/ml G-418 sulfate (Invitrogen) every third passage to select for the T7 polymerase-expressing cells. BEAS-2B cells, a human lung/bronchial epithelial cell line, were obtained from ATCC and grown in BEGM medium with all the recommended supplements (Lonza, Basel, Switzerland). Wild-type recombinant HMPV (rHMPV) strain CAN97-83, a genotype group A2 virus, kindly provided by Peter Collins and Ursula J. Buchholz (NIAID, Bethesda, MD), was propagated in Vero cells as previously described (6).

Plasmids. The HMPV SH gene was amplified from viral RNA preparations of the wild-type recombinant HMPV strain CAN97-83 and ligated into the pCAGGS mammalian expression vector, and a hemagglutinin (HA) tag was inserted at either the N or C terminus. HMPV F and G genes were kindly provided by Ursula J. Buchholz (NIAID, Bethesda, MD) and subcloned into pCAGGS (32). The plasmids pCAGGS-SV5 F and pCAGGS-SV5 HN were provided by Robert Lamb (Howard Hughes Medical Institute, Northwestern University, Evanston, IL). The truncation mutants SH-Ex and SH-In were constructed by amplifying, respectively, the extracellular and intracellular domain, including the transmembrane domain (TMD) of SH, with an HA tag inserted either N-terminal to the TMD for SH-Ex or C-terminal to the TMD for SH-In. For the analytical ultracentrifugation, the TMD sequence LIALKLILALL TFFTITITINYI (residues 31 to 53) was cloned downstream of the staphylococcal nuclease (SN) gene, as previously described (33). All constructs were sequenced in their entirety.

Expression, metabolic labeling, and biotinylation of surface proteins. COS-7 or Vero cells were transiently transfected with pCAGGS expression vectors using FuGene 6 (Roche, Basel, Switzerland) or Lipofectamine 2000 (Invitrogen). At 18 h posttransfection, the cells were starved, metabolically labeled with Tran^{35}S-label (100 μCi/ml; PerkinElmer, Waltham, MA), and either lysed or subjected to surface biotinylation prior to lysis, as previously described (33). Antipeptide serum to HMPV F or G (32) or the monoclonal Ab 12CA5 to the HA tag (Roche) was used to immunoprecipitate the desired proteins as previously described (34). Biotin-labeled protein was pulled down with immobilized streptavidin (Thermo Scientific, Rockford, IL), as described previously (33). Immunoprecipitated proteins were analyzed via SDS-15% polyacrylamide gel electrophoresis (SDS-PAGE) and visualized using the Typhoon imaging system (Amersham Biosciences/GE Healthcare Life Sciences, New Jersey). All Typhoon images were processed in Adobe Photoshop, with adjustments made equally to all portions of the image.

EndoH/PNGase treatment. COS-7 cells were transfected, metabolically labeled for 4 h, and chased for 1 h as described above. Immunoprecipitated proteins were digested with 0.5 μl of *N*-glycosidase F (PNGase F; Sigma) or 0.25 μl of endoglycosidase H (endoH; Roche) as previously described (35). The resulting proteins were analyzed via SDS-PAGE and visualized using the Typhoon imaging system.

Cross-linking. COS-7 or BSR cells were transfected and metabolically labeled for 4 h as described above. Cells were then detached from their plates with 1 ml of phosphate-buffered saline (PBS) with EDTA and subjected three times to centrifugation at 1,000 × *g* for 5 min with PBS washes in between. Cells were then resuspended in PBS, divided into two equal populations, and treated with 4 μl of 10% NP-40 at 4°C. One population was concomitantly treated with 4 μl of fresh 100 mM 3,3′-dithiobis[sulfosuccinimidylpropionate] (DTSSP) cross-linker (Thermo Scientific). After 1 h of treatment, DTSSP was quenched by the addition of glycine to a final concentration of 50 mM. Samples were lysed, and HA-tagged proteins were immunoprecipitated as described above.

Recombinant protein expression, purification, and analytical ultracentrifugation. Recombinant protein containing the TMD of HMPV SH fused to SN in pET-11a was expressed in Rosetta-gami cells (EMD Chemicals, Gibbstown, NJ) and purified as previously described (33). The purified protein, present in a solution containing 200 mM NaCl, 20 mM Na_2HPO_4-NaH_2PO_4 (pH = 7), 29% D_2O, and the Zwittergent detergent C14SB (Sigma/Fluka, St. Louis, MO) (36), was then used for sedimentation equilibrium analysis at three protein concentrations and three rotor speeds (20K, 25K, and 30K rpm) using a Beckman XL-A analytical ultracentrifuge (Beckman, Fullerton, CA) equipped with an An-60 Ti rotor at 25°C, as previously described (33, 37). The monomer molecular mass and the partial specific volumes were calculated using SEDNTERP (http://sednterp.unh.edu), and the equilibrium profiles were analyzed as previously described (33, 37) using KaleidaGraph (Synergy Software, Reading, PA) and HeteroAnalysis (38). The best fit was chosen based on the smallest square root of the variance (SRV) at the three concentrations and three speeds tested. Protein concentrations were determined by spectrophotometry, using E_{280} = 17,420 M^{-1} cm^{-1}.

Permeability test. COS-7 or Vero cells were transfected using Fugene 6. The day after transfection, cells were starved in Cys-Met-DMEM in the presence or absence of 500 μg/ml hygromycin B (Sigma) for 45 min. Cells

were subsequently labeled with Tran^{35}S for 1, 2, or 3 h in the presence or absence of 500 μg/ml hygromycin B. After being labeled, the indicated proteins were immunoprecipitated as described previously (32).

Cell cytotoxicity test. Vero or COS-7 cells were plated in a 96-well plate to allow processing of quadruplicate samples. The following day, cells were transfected with HMPV F, SH-HA, or HA-SH (empty vector as the control). The next day, cells were washed and a mix of 80 μl of Opti-MEM and 20 μl of cell titer solution was added according to the manufacturer's instructions (Promega, Madison, WI). The absorbance of each well was measured every 10 min using μQuant (Bio-Tek Instruments Inc., Winooski, VT) until the optical density (OD) reached 1.0.

Cell tracker staining. COS-7 cells were transfected using Fugene 6. Twenty-four hours posttransfection, cells were washed once with PBS and incubated with 10 μM CellTracker green 5-chloromethylfluorescein diacetate (CMFDA) (Molecular Probes) in prewarmed culture medium for 45 min at 37°C. After incubation, the staining solution was removed and the cells were washed once with culture medium and incubated for an additional 30 min at 37°C. Cells were then washed with PBS, fixed with 3.7% formaldehyde for 15 min at room temperature, and processed for immunofluorescence as described below. A secondary goat anti-mouse antibody conjugated with tetramethyl rhodamine isocyanate (TRITC) was used to detect HA-tagged HMPV SH protein.

Syncytium assay. Syncytium assays were performed as previously described (6, 32) using COS-7 or Vero cells in 6-well plates transiently transfected with a total of 4 μg of DNA using FuGene 6 (Roche) according to the manufacturer's instructions. The following morning, cell monolayers were treated with 0.3 μg/ml TPCK (L-1-tosylamide-2-phenylethyl chloromethyl ketone)-trypsin for 1 to 2 h and rinsed, and PBS [pH 5 or 7, buffered with 10 mM HEPES and 5 mM 2-(*N*-morpholino)ethanesulfonic acid (MES) hemisodium salt] was added for 4 min. Opti-MEM with 0.3 μg/ml TPCK-trypsin was then readded to the cells, and the pH pulse was repeated three more times (2 to 3 h apart). Cells were incubated overnight at 33°C, and digital photographs were taken the next morning with a Spot Insight FireWire digital camera mounted on a Carl-Zeiss Axiovert 100-invested microscope using a 10× objective (Thornwood, NY).

Reporter gene assay. COS-7 or Vero cells were plated in 60-mm dishes and transfected using FuGene 6 (Roche) with 2 μg of the T7 control plasmid (Promega) containing luciferase cDNA under the control of the T7 promoter and 3.5 μg plasmid DNA containing the viral glycoprotein expression constructs, as indicated. The following day, cells were overlaid onto BSR cells, which constitutively express the T7 polymerase (39). The combined cells were incubated at 37°C for 1 h and rinsed once with PBS (pH 7.2), and then PBS of the indicated pH buffered with 10 mM HEPES and 5 mM MES was added for 4 min at 37°C. The medium was replaced by Opti-MEM with 0.3 μg/ml TPCK-trypsin, and the cells were incubated at 37°C for 2 h. Two additional buffered PBS treatments were performed 2 h apart, and then the cells were incubated in DMEM with FBS at 37°C for 4 h to allow expression of luciferase, as previously determined (32). Finally, cell lysates were analyzed for luciferase activity using a luciferase assay system (Promega) according to the manufacturer's protocol. Light emission was measured using an Lmax luminometer (Molecular Devices, Sunnyvale, CA) (6).

Confocal microscopy. COS-7 or BEAS-2B cells were plated in 6-well dishes containing coverslips. Cells were transfected 24 h later with 2 μg of DNA encoding the SH constructs and 6 μl of FuGene 6. The day after, cells were exposed to HMPV (multiplicity of infection [MOI] = 5) for 2 h and subsequently incubated overnight. Cells were washed and fixed the next morning with 4% paraformaldehyde for 15 min at room temperature followed by permeabilization with 1% Triton X-100 for 15 min at 4°C. The HA-tagged proteins were detected using a primary monoclonal antibody directed against HA (Roche) and a secondary goat anti-mouse antibody conjugated with fluorescein isothiocyanate (FITC). HMPV M protein was detected using an antibody against the avian metapneumovirus C M protein, kindly provided by Sagar M. Goyal (University of Minnesota, Minneapolis, MN), which has been shown to cross-react with HMPV M (40), and a secondary goat anti-rabbit antibody conjugated with TRITC. Pictures were taken using the Nikon 1A confocal microscope and analyzed with the NIS-Elements software. Images were processed in Adobe Photoshop, with equivalent adjustments made to all panels.

RESULTS

Expression and modification of HMPV SH. To examine HMPV SH expression and localization, the HA tag coding sequence was inserted at the N terminus (HA-SH) or C terminus (SH-HA) of the SH gene, present in the pCAGGS mammalian expression vector (41). In addition, to analyze the role of the intracellular or extracellular domain, respectively, the extracellular (SH-In) or intracellular (SH-Ex) domain was replaced by the HA tag (Fig. 1A). Optimal expression of the different constructs was obtained in COS-7 cells (Fig. 1B). Immunoprecipitation of metabolically labeled proteins with an antibody to the HA tag resulted in specific bands for SH-HA or HA-SH at approximately 20 kDa (expected unglycosylated size of 21.5 kDa; Fig. 1B), and higher-molecular-mass bands were consistent with previous reports (18, 21) and likely represented glycosylated or oligomeric forms (SH_g and SH_x). The predominant form for SH-In corresponded to that expected for the unglycosylated monomer (approximately 7 kDa), consistent with removal of the potential glycosylation sites in the extracellular domain. SH-Ex was detected at low levels at the expected size (18 kDa). Surface biotinylation experiments (Fig. 1C) verified that both full-length HA-tagged SH forms were present on the cell surface, though the level of surface-expressed HA-SH was lower, suggesting that the presence of the HA tag on the cytoplasmic tail may affect folding and/or trafficking. To determine if the observed higher-molecular-mass forms were a result of *N*-linked glycosylation, removal of *N*-glycans by treatment with either EndoH or *N*-glycosidase F (PNGase F) was performed (32, 42). Treatment with either enzyme resulted in a loss of the SH_g form, confirming that this species contained *N*-linked glycans (Fig. 1D). Interestingly, several bands corresponding to high-molecular-mass forms appeared after *N*-glycan removal (Fig. 1D, arrows), potentially representing oligomeric species.

Cellular localization of HMPV SH. To confirm surface localization of HMPV SH, examine intracellular localization, and determine if infection state influenced SH cellular distribution, BEAS-2B cells, derived from human bronchial epithelium, were transfected with pCAGGS SH-HA or HA-SH. Twenty-four hours posttransfection, the cells were infected with HMPV and then fixed and permeabilized the following day. Immunofluorescence analysis was performed with a primary antibody against HA (Fig. 2). Consistent with the biotinylation results (Fig. 1C), HMPV HA-SH and SH-HA were partially detected on the plasma membrane, but internal localization was also observed (Fig. 2A and C). Coinfection with HMPV did not result in significant alteration of SH cellular localization (Fig. 2B and D), suggesting that the presence of other viral proteins is not critical for SH localization. Similar results were observed with COS-7 cells (data not shown).

HMPV SH forms higher-order oligomers in a process at least partially driven by the transmembrane domain. Initial analysis (Fig. 1) suggested the presence of higher-order oligomeric forms of HMPV SH. To more closely analyze SH oligomerization, HA-SH- or SH-HA-expressing BSR cells were metabolically labeled and subjected to DTSSP cross-linking. DTSSP addition (Fig. 3A, right) resulted in a decrease in the SH and SH_g bands and a large

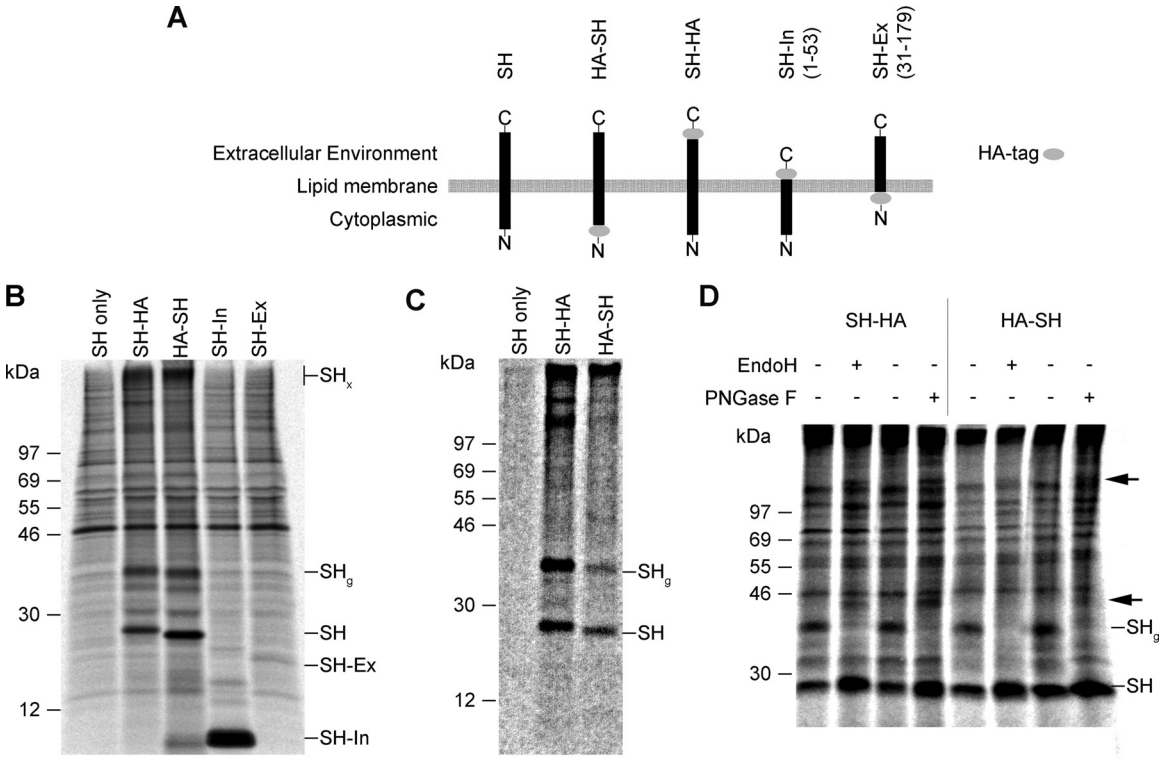

FIG 1 HMPV SH constructs tagged with HA are expressed at the surface of COS-7 cells in their glycosylated forms. (A) Schematic diagram of SH constructs used in this study. For SH-In and SH-Ex, amino acid residues present in wild-type SH are indicated in parentheses. Black, SH protein; gray oval, HA tag. (B) Total expression of HMPV SH constructs tagged with HA. COS-7 cells transfected with plasmids encoding wild-type SH (SH only), SH tagged at the C terminus (SH-HA), SH tagged at the N terminus (HA-SH), the SH intracellular domain/TM tagged with HA (SH-In), and the SH extracellular domain/TM tagged with HA (SH-Ex) were metabolically labeled and immunoprecipitated prior to analysis by SDS-PAGE. Multiple bands were detected, including those corresponding, in predicted migration, to SH monomer (SH), glycosylated SH (SH_g), and some higher-molecular-mass species (SH_x). (C) Surface expression of HMPV SH, SH-HA, and HA-SH in COS-7 cells. Metabolically labeled cell surface proteins were biotinylated, isolated using streptavidin beads, and analyzed by SDS-PAGE. (D) HA-tagged constructs of HMPV SH expressed in COS-7 cells were immunoprecipitated and digested with EndoH or PNGase prior to analysis by SDS-PAGE. Digestion with EndoH or PNGase abolished the presence of the glycosylated form of SH (SH_g) and led to the appearance of several new higher-molecular-mass forms (arrows). All images shown are representative of at least four independent experiments.

increase in higher-molecular-mass forms which migrated near the top of the gel. Similar results were observed for SH expression in COS-7 cells (data not shown). These results suggest that HMPV SH forms higher-order oligomeric species, with the broad band potentially due to the presence of several oligomeric species and/or diversity in the attached glycans. RSV SH has been demonstrated to homo-oligomerize as a pentamer and/or hexamer (25, 27–29), and this oligomerization has been proposed to be critical for viroporin activity (26). Viroporin oligomerization has been suggested to involve transmembrane or hydrophobic domain interactions (23, 28, 29). To analyze the capacity of the HMPV SH transmembrane domain to self-associate, we constructed chimeric proteins containing the staphylococcal nuclease (SN) protein linked to the transmembrane domain of HMPV SH. SN is a monomeric protein under the conditions utilized for sedimentation equilibrium analytical ultracentrifugation (43), allowing for determination of the transmembrane domain association by identification of oligomeric species. The SN-SH TM chimeric protein was expressed, purified, and exchanged into C14SB to density match the detergent to the buffer, thus allowing the analysis of the mass of the protein species separate from the mass of the surrounding detergent micelles (33, 37). Analysis of a chimeric protein containing the HMPV SH TMD region (residues 31 to 53) at three concentrations and speeds indicated that monomer-heptamer or monomer-octamer (Fig. 3B) were the best-fit models, indicating that the transmembrane domain forms a large oligomeric species. The small, symmetrically distributed residuals (upper panels in Fig. 3B) indicated that the monomer-octamer model was consistent with the mass distributions present. These results indicate that the HMPV SH protein transmembrane domain, separate from the rest of the protein, can form higher-order oligomers, consistent with reported characteristics of viroporins.

HMPV SH expression increases cell permeability to hygromycin B. To directly test whether HMPV SH expression can alter membrane permeability, we utilized hygromycin B, an antibiotic which blocks cellular protein translation but which does not efficiently penetrate the plasma membrane when present at low concentrations (30, 31, 44, 45). COS-7 cells transiently expressing HMPV F (as a control), HMPV SH-HA, or HMPV HA-SH were metabolically labeled for 1, 2, or 3 h in the presence or absence of 500 μg/ml hygromycin B. To analyze effects on protein synthesis in only the transfected cells, the HMPV F protein or the HA-tagged SH proteins were purified by immunoprecipitation, and the level of newly synthesized proteins was determined by SDS-PAGE followed by imaging and quantitation on the Typhoon. A minor reduction in protein synthesis was observed in the HMPV F

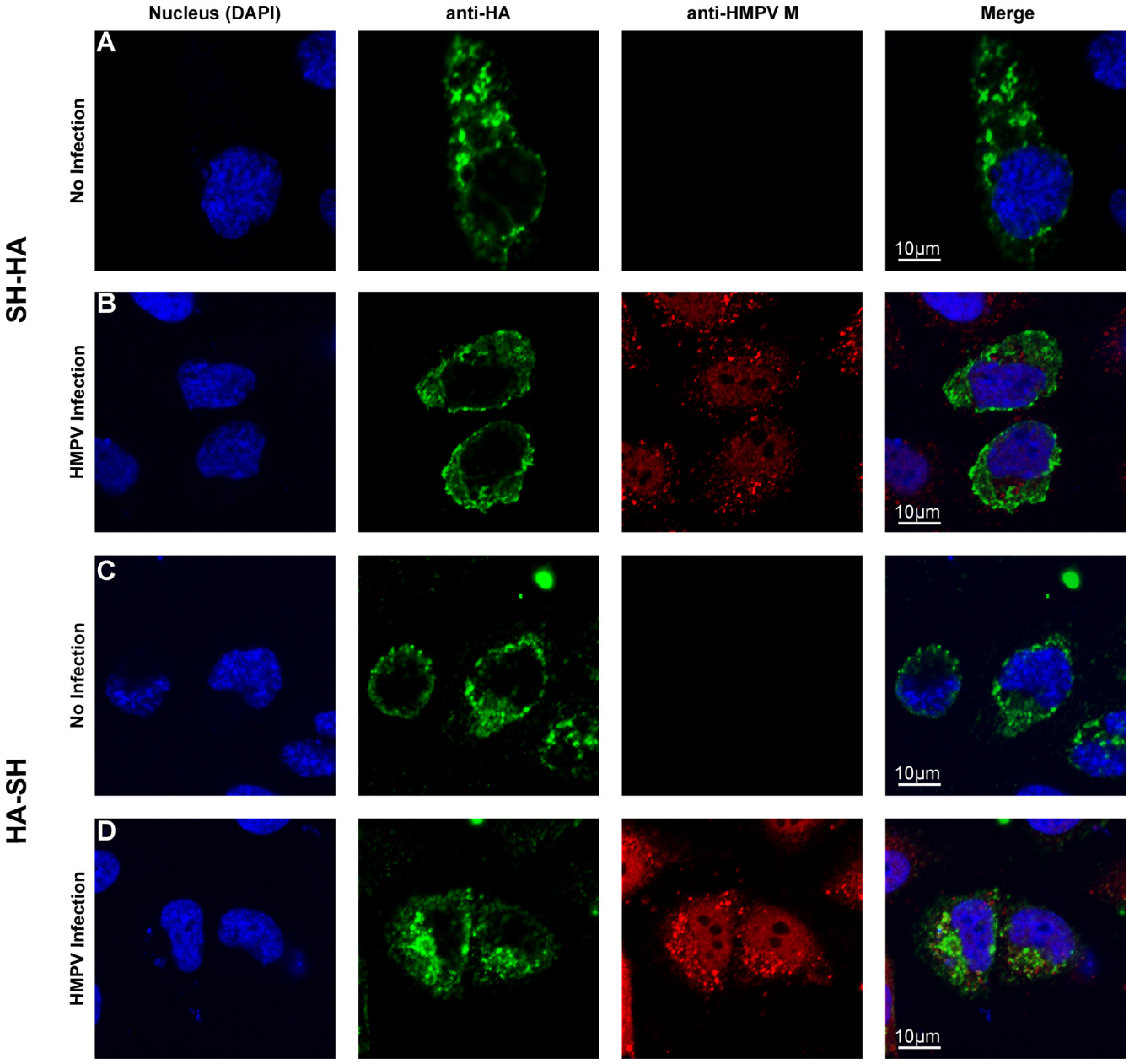

FIG 2 HMPV SH localizes to plasma membrane and intracellular organelles. BEAS-2B cells transfected with plasmids encoding HA-tagged HMPV SH were infected with HMPV 24 h posttransfection. The following day, cells were fixed and stained with an anti-HA antibody followed by a FITC-conjugated secondary antibody (green) and an antibody that recognizes HMPV M followed by a TRITC-conjugated secondary antibody (red). DAPI (4′,6-diamidino-2-phenylindole) stain was used to stain the cell nucleus (blue). Control images of cells expressing HA-tagged HMPV SH in the absence of HMPV infection are also shown. Images are representative of 3 independent experiments.

control (approximately 15% with 1 h of hygromycin B treatment). However, expression of SH-HA or HA-SH (Fig. 4A) reduced cellular protein synthesis to a much greater extent. Protein expression was further decreased with 2 or 3 h of hygromycin B treatment. These results indicate that expression of the HMPV SH protein increases cell permeability to small compounds, consistent with HMPV SH potentially functioning as a viroporin.

HMPV SH expression does not affect cell viability. To verify that the decrease in protein synthesis observed with hygromycin B treatment was not a result of a general decrease in cell viability, the effect of HMPV SH expression on viable cell number was measured using a CellTiter 96 assay (Promega). Vero and COS-7 cells were transfected with pCAGGS constructs expressing HMPV F, HMPV SH, the HA-tagged SH constructs, or empty vector as the control (Fig. 4B). Forty-eight hours posttransfection, the OD at 490 nm was measured every 10 min. The average slope of the OD increase was calculated and normalized to the slope observed with cells transfected with empty vector. No significant difference in the number of viable cells was observed with any of the viral proteins, indicating that transient expression of HMPV SH does not

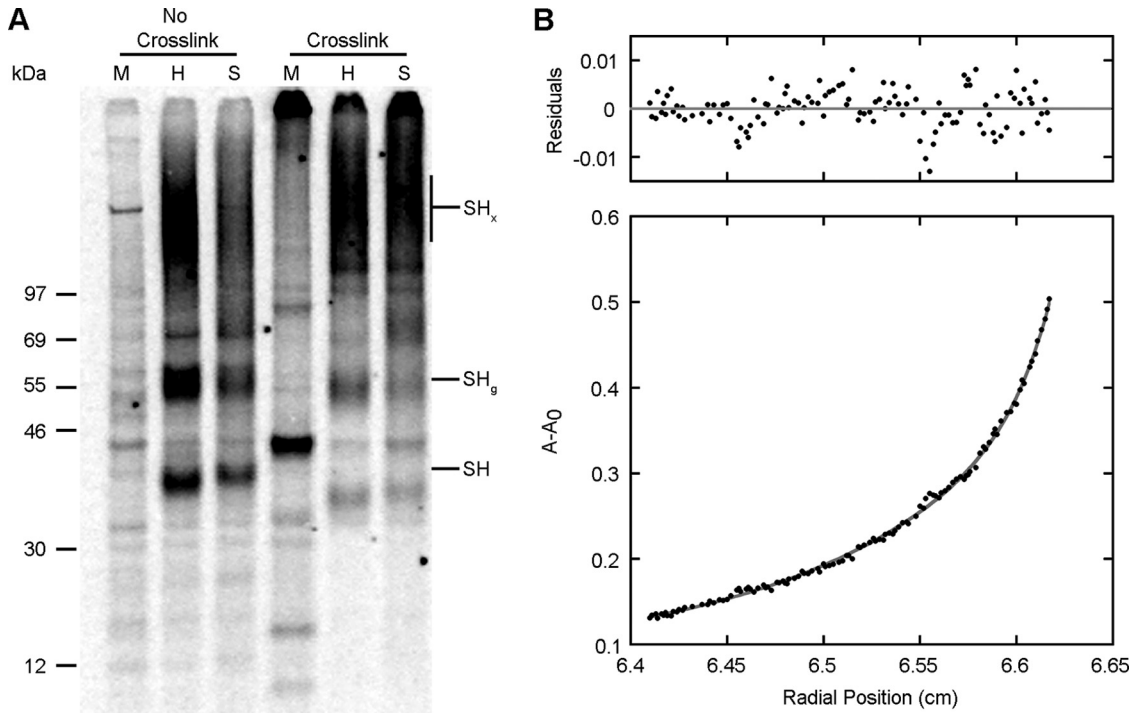

FIG 3 The transmembrane domain of HMPV SH promotes oligomerization of the SH protein. (A) BSR cells expressing HA-tagged HMPV SH at the N- and C-terminal ends (S and H, respectively) were radiolabeled, treated with DTSSP in the presence of 0.16% NP-40, and analyzed using a 4 to 12% Bis-Tris gel following immunoprecipitation using an anti-HA affinity matrix as previously described. The figure shown is representative of 3 independent experiments. M, empty vector control; H, HA-SH; S, SH-HA. (B) Sedimentation equilibrium analysis for the SN-SH TMD construct. Data points are shown with the fit for a monomer-octamer equilibrium (fitted curve in gray). $\chi^2 = 0.0016689$ and $R = 0.9992$.

alter cell viability. Similar analysis was performed on cells infected with wild-type HMPV or with mutant viruses lacking the HMPV G or both HMPV G and SH proteins, and no significant difference in cell viability was observed (data not shown), again indicating that the presence of HMPV SH does not significantly alter overall cell viability.

HMPV SH expression alters intracellular localization of a fluorescent dye. Incubation of cells with CellTracker green CMFDA, which is processed to a membrane-impermeable fluorescent form, generally results in low-level fluorescence throughout the cytoplasm and nucleus (Fig. 5A and B, MCS). Interestingly, cells expressing either HA-tagged form of the HMPV SH protein displayed significantly different CellTracker green staining patterns. A more intense signal was observed in cells expressing the HA-tagged SH compared to in cells that did not (Fig. 5A). In addition, the fluorescent signal was dramatically relocalized to discrete structures near the plasma membrane, potentially consistent with intracellular vesicles or endosomes (Fig. 5B, SH-HA and HA-SH). Immunofluorescence studies (Fig. 2 and 5) indicate that the HMPV SH protein is present both intracellularly and on the plasma membrane, and the alterations of CellTracker localization are consistent with SH-promoted alterations in membrane permeability in both locations.

HMPV SH inhibits fusion mediated by HMPV F. As HMPV SH is partially present on the cell surface and can alter membrane permeability, we next examined the effect of HMPV expression on membrane fusion promoted by the HMPV F protein or other paramyxovirus fusion proteins. A reporter fusion assay was performed as previously described (32). Interestingly, expression of wild-type HMPV SH or either HA-tagged form inhibited HMPV F-promoted membrane fusion to the background levels seen with the attachment protein alone (Fig. 6A, HMPV). A more modest decrease in fusion was observed when wild-type HMPV SH or the HA-tagged forms were coexpressed with parainfluenza virus 5 (PIV5) F and HN (Fig. 6A, PIV5) or Hendra F and G (Fig. 6A, Hendra), indicating that some nonspecific inhibition of fusion is also observed. To evaluate the role of differing domains of SH in fusion inhibition, the effect of coexpression of SH-In and SH-Ex with HMPV F was analyzed (Fig. 6B). While inhibition of fusion was observed with both, SH-Ex coexpression resulted in a significantly greater inhibition, suggesting that the transmembrane domain and extracellular region play the greatest role in the effect of SH on membrane fusion. To verify that these results were not assay specific, syncytial assays were performed to analyze the effect of SH and the SH deletions on HMPV F-mediated fusion (Fig. 6C) and Hendra F/G- and PIV5 F/HN-mediated fusion (data not shown). Syncytial results confirmed the inhibitory effect of HMPV SH on membrane fusion and the importance of the transmembrane domain/extracellular region in this process.

SH coexpression does not significantly reduce viral glycoprotein surface expression. Membrane fusion promoted by viral fusion proteins is strongly affected by glycoprotein surface expression. To verify that SH expression did not inhibit fusion by altering glycoprotein surface expression, biotinylation of HMPV F and G in the presence or absence of the SH constructs was assessed. HMPV F (Fig. 7A) and HMPV G (Fig. 7B) were properly expressed on the cell surface in the presence or absence of the various SH constructs, and cleavage of the HMPV F_0 precursor form to the

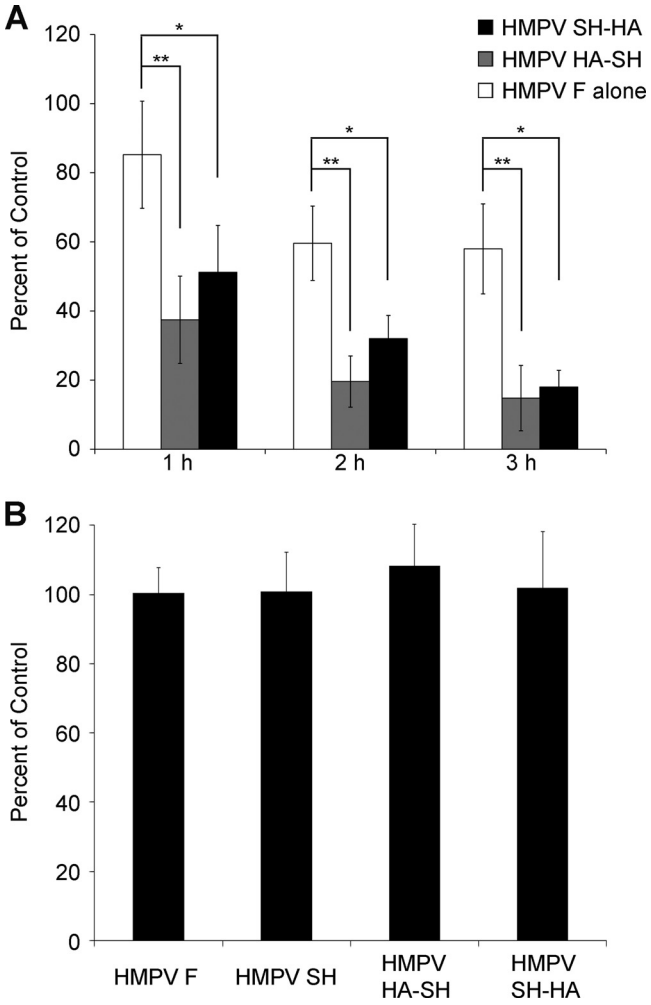

FIG 4 HMPV SH increases permeability of cellular membranes without affecting the cellular viability. (A) COS-7 cells transfected with plasmids encoding either the HMPV F protein or an HA-tagged HMPV SH protein were treated with 500 μg/ml of hygromycin (no treatment as the control) and subsequently radiolabeled for 1, 2, or 3 h in the presence or absence of hygromycin. The HMPV F or SH protein was immunoprecipitated and analyzed by SDS-PAGE. The signal intensity of the band for samples treated with hygromycin was normalized to the signal of the untreated samples at the corresponding time point ($n = 3$). White, HMPV F alone; gray, HMPV HA-SH; black, HMPV SH-HA. Significance was analyzed by Student's t test and is indicated by asterisks (*, $P < 0.09$; **, $P < 0.05$). Error bars = standard errors of the means (SEM). (B) Metabolic activity of COS-7 cells in 96-well plates transfected with empty pCAGGS or pCAGGS encoding the HMPV F or the HMPV SH constructs SH-HA, HA-SH, or SH WT was measured as described in Materials and Methods. Formazan production was measured at 10-min intervals until the OD of control samples (empty pCAGGS) reached 1. Graph represents the average OD slope increase normalized to HMPV G from four independent experiments ($n = 4$) performed in quadruplicates. Statistical differences were analyzed by analysis of variance (ANOVA).

F_1 and F_2 fusion active form was not altered by SH expression (Fig. 7A). Quantitation of four independent experiments indicated that no significant difference in HMPV F surface expression was observed when wild-type SH or the HA-tagged SH versions were present (Fig. 7C). Interestingly, radiolabeled SH-HA, HA-SH, wild-type SH, and SH-Ex were observed to coimmunoprecipitate with HMPV F (Fig. 7A), whereas no coimmunoprecipitation was observed with HMPV G. These results indicate that HMPV F-mediated fusion inhibition by HMPV SH is not due to alterations in the levels of HMPV F surface expression or proteolytic activation and suggest a potential interaction between the two proteins.

DISCUSSION

All primary HMPV isolates to date contain an SH gene (19, 20), suggesting an important function for viral fitness, but the specific role of the HMPV SH protein remains unclear. HMPV SH is dispensable for growth in cell culture (18), and a recombinant virus lacking the SH gene gave only a minor reduction in viral replication in a nonhuman primate model (7), indicating that the effect of SH may be tightly species dependent. HMPV SH has been suggested to alter NF-κB transcriptional activity, leading to enhanced secretion of proinflammatory cytokines (21), but no significant differences in expression of these genes was detected with microarray analysis (22). Our studies provide insight into two potential functions of HMPV SH: membrane permeabilization, or viroporin-like activity, and modulation of fusion protein activity.

A number of viruses have been shown to encode small proteins capable of altering membrane permeability, or viroporins (23). A series of studies have shown that the SH protein from RSV, a closely related virus, may function as a viroporin, and our results suggest important parallels with HMPV SH. RSV SH has been shown to permeabilize membranes (24, 29), and our studies indicate that expression of HMPV SH increases permeability of cell membranes to hygromycin B (Fig. 4A) and alters intensity and localization of CellTracker green (Fig. 5). RSV SH is localized both to intracellular compartments, including the Golgi, and to the plasma membrane (46), and similar cellular distribution was observed for HMPV SH (Fig. 2). A Flag-tagged RSV SH was shown to form ringlike multimers (29), and both the entire RSV SH protein (26) and its transmembrane domain region (25) have been shown to form pentamers. Our work demonstrates that the HMPV SH protein forms higher-order oligomers (Fig. 3A) and that the HMPV SH transmembrane domain alone is sufficient to drive oligomerization to large multimers (Fig. 3B). RSV SH has recently been shown to form a pH-sensitive ion channel (26), and further research will be needed to determine if the HMPV SH protein has a similar function. A recent study supports a role for the RSV SH viroporin function in inflammasome activation (47), but the potential role of a viroporin in the HMPV life cycle also remains to be elucidated.

HMPV SH has been detected in viral particles both by Western blot analysis (18, 22, 48) and by mass spectrometry analysis (22). We performed similar liquid chromatography-tandem mass spectrometry (LC-MS/MS) analysis on virions generated from Vero, COS-7, or LLCMK2 cells which had been purified through two sucrose cushions and two sucrose gradients. Peptides corresponding to HMPV F could be readily detected in all virion preparations. Peptides corresponding to HMPV G were detected in virions prepared from Vero or COS-7 cells, but significant detection of HMPV G in virions purified from LLC-MK2 cells required removal of *O*-linked glycans, suggesting that the extent of *O*-linked glycosylation for HMPV G may vary in viruses prepared from different cell types. Interestingly, SH-specific peptides were not observed in any virion preparations, even with prior *O*-linked glycan removal (data not shown). These results suggest that the level of HMPV SH incorporated into virions is extremely low compared to that of the other HMPV glycoproteins. A small

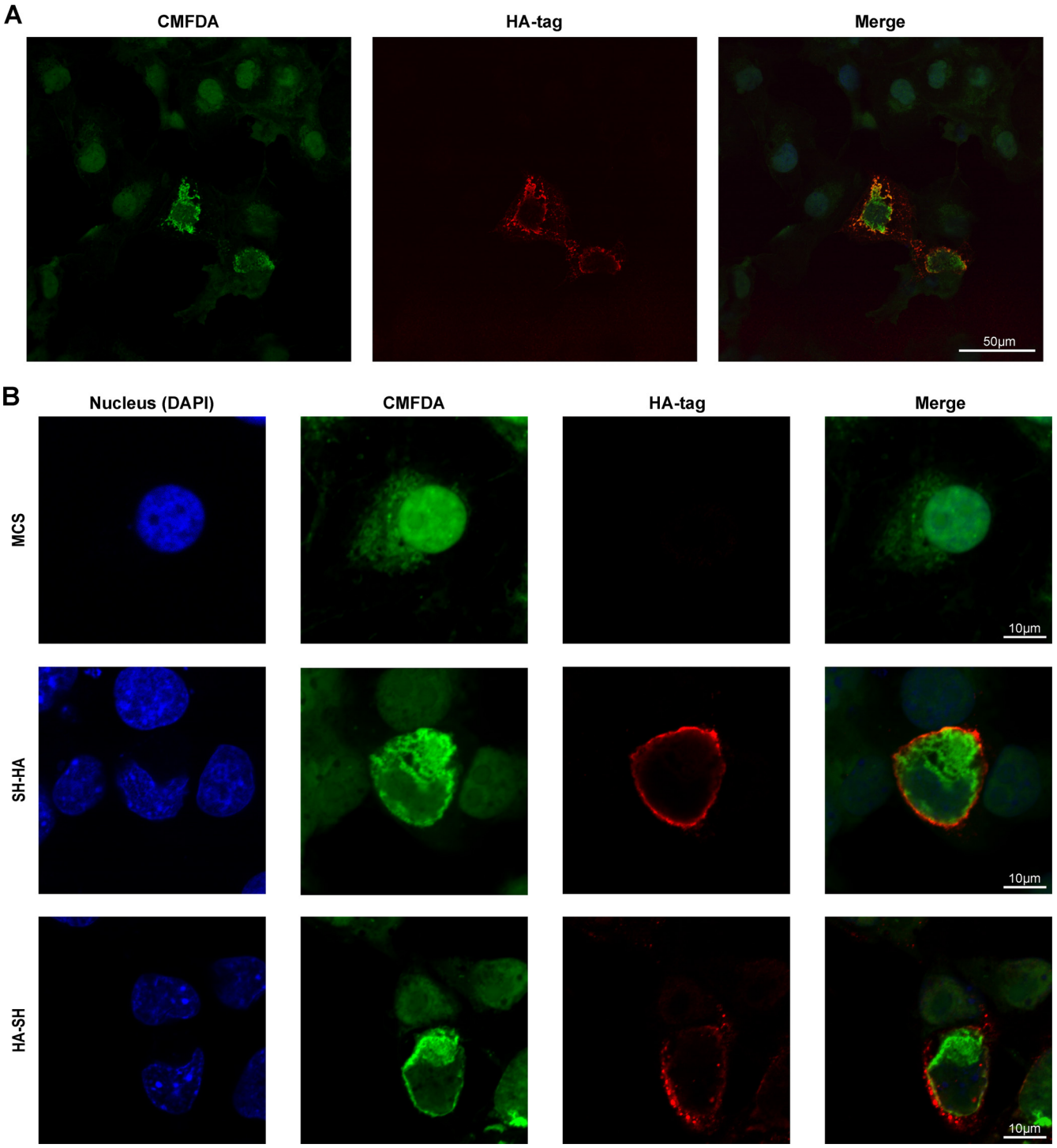

FIG 5 HMPV SH alters membrane permeability to a fluorescent dye. (A) COS-7 cells were transfected with a plasmid encoding an HA-tagged HMPV SH protein, and 24 h posttransfection, cells were incubated with 10 μM CellTracker CMFDA for 30 min at 37°C. Cells were then incubated for an additional 30 min in culture medium, fixed with 3.7% formaldehyde, and stained with an anti-HA antibody followed by a TRITC-conjugated secondary antibody (red). (B) COS-7 cells were transfected with empty plasmid or plasmids encoding HA-tagged HMPV SH protein and processed as described for panel A. DAPI stain was used to stain the cell nucleus (blue).

amount of RSV SH has been reported in RSV filaments (46), and the influenza M2 ion channel is incorporated in small amounts onto the viral particles (49, 50), suggesting that the level of proteins which modulate membrane permeability may need to be tightly regulated.

Interestingly, our studies also indicate that expression of the HMPV SH protein can inhibit fusion protein function. Coexpression of HMPV SH, either untagged or SH tagged on either termini, resulted in an approximately 90% decrease in HMPV F-promoted membrane fusion as judged by a reporter gene assay (Fig. 6A), and

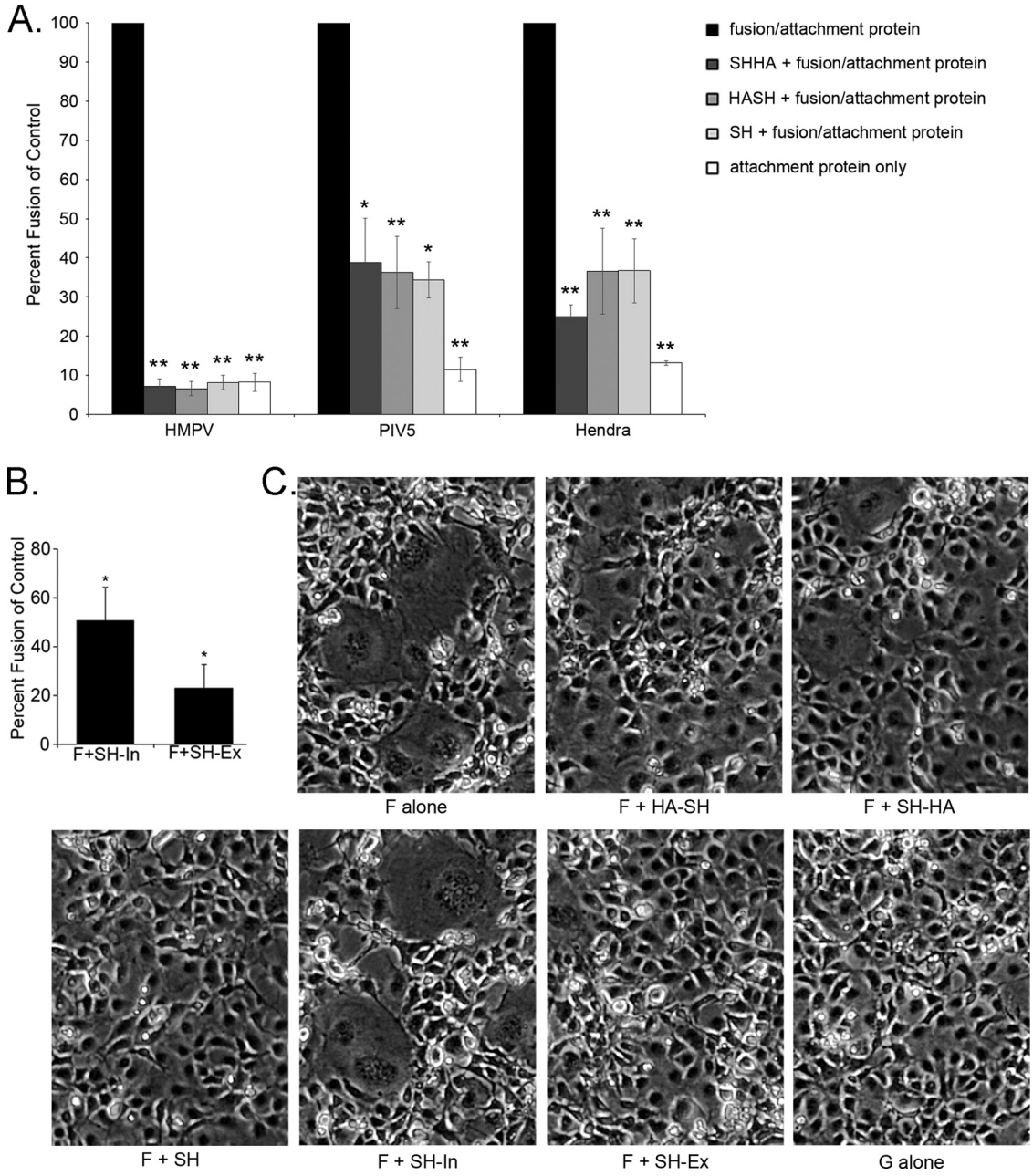

FIG 6 HMPV SH decreases fusogenic activity of paramyxovirus F proteins. (A) Luciferase reporter gene fusion assay of COS-7 cells transfected with either HMPV F or G alone, Hendra G alone or in combination with Hendra F, and PIV5 HN alone or in combination with PIV5 F in conjunction with plasmids encoding the above-mentioned HMPV SH constructs was performed as described. Data presented are normalized against luminosity at pH 5 for HMPV F alone, PIV5 F and HN, and Hendra F and G. Significance compared to WT was analyzed by ANOVA and is indicated by asterisks (*, $P < 0.001$; **, $P < 0.005$). Error bars = SEM. (B) Fusogenic activity of COS-7 cells transfected with plasmids encoding HMPV F and constructs of HMPV SH devoid of the extracellular (SH-In) or intracellular (SH-Ex) domains was assessed as described for panel A. Data presented are normalized against luminosity of HMPV F alone at pH 5 ($n = 3$). Significance compared to WT was analyzed by ANOVA and is indicated by asterisks (*, $P < 0.05$). (C) Representative images ($n = 3$) of syncytium production of COS-7 cells transfected with plasmids encoding HMPV F WT and the different HMPV-SH constructs after four brief pH 5 pulses.

this fusion inhibition was confirmed in syncytial assays (Fig. 6C). This decrease is not due to alterations in the surface expression of the glycoproteins (Fig. 7), suggesting an effect of HMPV SH on the membranes or proteins involved in the fusion process. HMPV SH coexpression also reduced fusion promoted by the PIV5 and Hendra F proteins (Fig. 6A), indicating that at least part of the inhibition may be nonspecific, potentially due to the ability of SH to alter membrane permeability. The much greater inhibition observed for HMPV F-promoted fusion suggests a specific effect, and our results indicate that the transmembrane domain and large extracellular domain are principally responsible (Fig. 6B). The HMPV SH protein, at 179 amino acids, is considerably larger than the 64-amino-acid RSV SH protein, and no specific function for the larger extracellular domain has been described. Our results

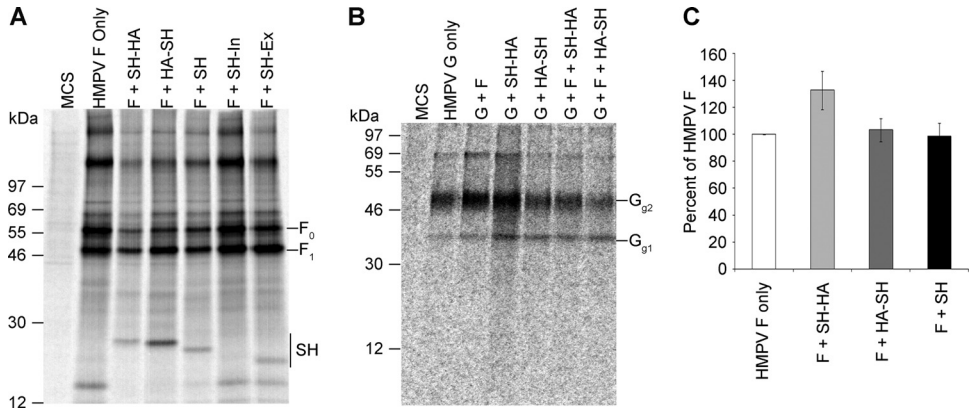

FIG 7 HMPV SH does not alter surface expression levels of HMPV F and G. COS-7 cells transfected with the HMPV F-, G-, or SH-encoding plasmids alone or in combination were radiolabeled and the surface proteins were biotinylated as described. HMPV F (A) or G (B) proteins were immunoprecipitated, and the surface population was isolated using streptavidin beads. Images are representative of 4 independent experiments. (C) Quantification of the intensity of the signal corresponding to HMPV F in panel A. No statistical significant difference of HMPV F expression level was detected in the presence of HMPV SH-HA or HA-SH (ANOVA; $n = 4$ experiments).

indicate that both the full-length SH protein and SH-Ex efficiently coimmunoprecipitate with HMPV F (Fig. 7A) but not with HMPV G (Fig. 7B), so it is possible that direct interactions between the SH ectodomain and the fusion protein can result in fusion inhibition.

While these results clearly demonstrate that HMPV SH can modulate membrane fusion promotion, the role this may play in HMPV infection remains to be determined. Vero cells infected with either wild-type HMPV or a mutant lacking both HMPV G and SH did not significantly differ in terms of number and/or size of syncytia (data not shown). The presence of other viral proteins may modulate the fusion inhibition by SH, restricting this function to certain times or locations during infection. Alternatively, the level of SH protein may be important for fusion inhibition, and this level may change throughout infection and may differ between infected and transfected cells. No information is currently available on the cellular expression level of HMPV SH during infection, but our experiments do indicate that the cellular localization of the HA-tagged forms of HMPV SH does not significantly change in the presence or absence of HMPV infection (Fig. 2). Future experiments will be needed to determine whether global or local alterations to SH concentrations may affect the function of the F protein at particular stages of the HMPV life cycle.

ACKNOWLEDGMENTS

We thank members of the Dutch lab for discussions and evaluations of experiments and of the manuscript. We thank Sagar M. Goyal (University of Minnesota, Minneapolis, MN) for the antibody to avian metapneumovirus C M protein, Ursula Buchholz and Peter Collins (National Institutes of Health) for providing key HMPV reagents, and Guy Boivin (Centre Hospitalier Universitaire de Québec, Quebec City, Quebec, Canada) for his permission to obtain HMPV. We also thank Haining Zhu, Jing Chen, and Carol Beach (University of Kentucky) for assistance with the mass spectrometry and Michael Fried (University of Kentucky) for assistance with sedimentation equilibrium centrifugation.

This work was supported by NIH grants R01AI051517 and 2P20 RR020171 from the National Center for Research Resources to R.E.D. and an AHA predoctoral fellowship to A.C.

REFERENCES

1. **Schildgen V, van den Hoogen B, Fouchier R, Tripp RA, Alvarez R, Manoha C, Williams J, Schildgen O.** 2011. Human metapneumovirus: lessons learned over the first decade. Clin. Microbiol. Rev. **24:**734–754. http://dx.doi.org/10.1128/CMR.00015-11.
2. **Williams JV, Edwards KM, Weinberg GA, Griffin MR, Hall CB, Zhu Y, Szilagyi PG, Wang CK, Yang CF, Silva D, Ye D, Spaete RR, Crowe JE, Jr.** 2010. Population-based incidence of human metapneumovirus infection among hospitalized children. J. Infect. Dis. **201:**1890–1898. http://dx.doi.org/10.1086/652782.
3. **Kahn JS.** 2006. Epidemiology of human metapneumovirus. Clin. Microbiol. Rev. **19:**546–557. http://dx.doi.org/10.1128/CMR.00014-06.
4. **Widmer K, Zhu Y, Williams JV, Griffin MR, Edwards KM, Talbot HK.** 2012. Rates of hospitalizations for respiratory syncytial virus, human metapneumovirus, and influenza virus in older adults. J. Infect. Dis. **206:**56–62. http://dx.doi.org/10.1093/infdis/jis309.
5. **van den Hoogen BG, de Jong JC, Groen J, Kuiken T, de Groot R, Fouchier RA, Osterhaus AD.** 2001. A newly discovered human pneumovirus isolated from young children with respiratory tract disease. Nat. Med. **7:**719–724. http://dx.doi.org/10.1038/89098.
6. **Chang A, Masante C, Buchholz UJ, Dutch RE.** 2012. Human metapneumovirus (HMPV) binding and infection are mediated by interactions between the HMPV fusion protein and heparan sulfate. J. Virol. **86:**3230–3243. http://dx.doi.org/10.1128/JVI.06706-11.
7. **Biacchesi S, Pham QN, Skiadopoulos MH, Murphy BR, Collins PL, Buchholz UJ.** 2005. Infection of nonhuman primates with recombinant human metapneumovirus lacking the SH, G, or M2–2 protein categorizes each as a nonessential accessory protein and identifies vaccine candidates. J. Virol. **79:**12608–12613. http://dx.doi.org/10.1128/JVI.79.19.12608-12613.2005.
8. **He B, Leser GP, Paterson RG, Lamb RA.** 1998. The paramyxovirus SV5 small hydrophobic (SH) protein is not essential for virus growth in tissue culture cells. Virology **250:**30–40. http://dx.doi.org/10.1006/viro.1998.9354.
9. **Jin H, Cheng X, Zhou HZ, Li S, Seddiqui A.** 2000. Respiratory syncytial virus that lacks open reading frame 2 of the M2 gene (M2-2) has altered growth characteristics and is attenuated in rodents. J. Virol. **74:**74–82. http://dx.doi.org/10.1128/JVI.74.1.74-82.2000.
10. **Karron RA, Buonagurio DA, Georgiu AF, Whitehead SS, Adamus JE, Clements-Mann ML, Harris DO, Randolph VB, Udem SA, Murphy BR, Sidhu MS.** 1997. Respiratory syncytial virus (RSV) SH and G proteins are not essential for viral replication *in vitro*: clinical evaluation and molecular characterization of a cold-passaged, attenuated RSV subgroup B mutant. Proc. Natl. Acad. Sci. U. S. A. **94:**13961–13966. http://dx.doi.org/10.1073/pnas.94.25.13961.
11. **Takeuchi K, Tanabayashi K, Hishiyama M, Yamada A.** 1996. The mumps virus SH protein is a membrane protein and not essential for virus growth. Virology **225:**156–162. http://dx.doi.org/10.1006/viro.1996.0583.
12. **Ling R, Sinkovic S, Toquin D, Guionie O, Eterradossi N, Easton AJ.** 2008. Deletion of the SH gene from avian metapneumovirus has a greater impact on virus production and immunogenicity in turkeys than deletion of the G gene or M2–2 open reading frame. J. Gen. Virol. **89:**525–533. http://dx.doi.org/10.1099/vir.0.83309-0.
13. **Bukreyev A, Whitehead SS, Murphy BR, Collins PL.** 1997. Recombinant

respiratory syncytial virus from which the entire SH gene has been deleted grows efficiently in cell culture and exhibits site-specific attenuation in the respiratory tract of the mouse. J. Virol. **71:**8973–8982.
14. **Whitehead SS, Bukreyev A, Teng MN, Firestone CY, St. Claire M, Elkins WR, Collins PL, Murphy BR.** 1999. Recombinant respiratory syncytial virus bearing a deletion of either the NS2 or SH gene is attenuated in chimpanzees. J. Virol. **73:**3438–3442.
15. **Li Z, Xu J, Patel J, Fuentes S, Lin Y, Anderson D, Sakamoto K, Wang LF, He B.** 2011. Function of the small hydrophobic protein of J. paramyxovirus. J. Virol. **85:**32–42. http://dx.doi.org/10.1128/JVI.01673-10.
16. **Wilson RL, Fuentes SM, Wang P, Taddeo EC, Klatt A, Henderson AJ, He B.** 2006. Function of small hydrophobic proteins of paramyxovirus. J. Virol. **80:**1700–1709. http://dx.doi.org/10.1128/JVI.80.4.1700-1709.2006.
17. **Olmsted RA, Collins PL.** 1989. The 1A protein of respiratory syncytial virus is an integral membrane protein present as multiple, structurally distinct species. J. Virol. **63:**2019–2029.
18. **Biacchesi S, Skiadopoulos MH, Yang L, Lamirande EW, Tran KC, Murphy BR, Collins PL, Buchholz UJ.** 2004. Recombinant human metapneumovirus lacking the small hydrophobic SH and/or attachment G glycoprotein: deletion of G yields a promising vaccine candidate. J. Virol. **78:**12877–12887. http://dx.doi.org/10.1128/JVI.78.23.12877-12887.2004.
19. **Ishiguro N, Ebihara T, Endo R, Ma X, Kikuta H, Ishiko H, Kobayashi K.** 2004. High genetic diversity of the attachment (G) protein of human metapneumovirus. J. Clin. Microbiol. **42:**3406–3414. http://dx.doi.org/10.1128/JCM.42.8.3406-3414.2004.
20. **van den Hoogen BG, Bestebroer TM, Osterhaus AD, Fouchier RA.** 2002. Analysis of the genomic sequence of a human metapneumovirus. Virology **295:**119–132. http://dx.doi.org/10.1006/viro.2001.1355.
21. **Bao X, Kolli D, Liu T, Shan Y, Garofalo RP, Casola A.** 2008. Human metapneumovirus small hydrophobic protein inhibits NF-kappaB transcriptional activity. J. Virol. **82:**8224–8229. http://dx.doi.org/10.1128/JVI.02584-07.
22. **de Graaf M, Herfst S, Aarbiou J, Burgers PC, Zaaraoui-Boutahar F, Bijl M, van Ijcken W, Schrauwen EJ, Osterhaus AD, Luider TM, Scholte BJ, Fouchier RA, Andeweg AC.** 2013. Small hydrophobic protein of human metapneumovirus does not affect virus replication and host gene expression *in vitro*. PLoS One **8:**e58572. http://dx.doi.org/10.1371/journal.pone.0058572.
23. **Gonzalez ME, Carrasco L.** 2003. Viroporins. FEBS Lett. **552:**28–34. http://dx.doi.org/10.1016/S0014-5793(03)00780-4.
24. **Perez M, Garcia-Barreno B, Melero JA, Carrasco L, Guinea R.** 1997. Membrane permeability changes induced in *Escherichia coli* by the SH protein of human respiratory syncytial virus. Virology **235:**342–351. http://dx.doi.org/10.1006/viro.1997.8696.
25. **Gan SW, Ng L, Lin X, Gong X, Torres J.** 2008. Structure and ion channel activity of the human respiratory syncytial virus (hRSV) small hydrophobic protein transmembrane domain. Protein Sci. **17:**813–820. http://dx.doi.org/10.1110/ps.073366208.
26. **Gan SW, Tan E, Lin X, Yu D, Wang J, Tan GM, Vararattanavech A, Yeo CY, Soon CH, Soong TW, Pervushin K, Torres J.** 2012. The small hydrophobic protein of the human respiratory syncytial virus forms pentameric ion channels. J. Biol. Chem. **287:**24671–24689. http://dx.doi.org/10.1074/jbc.M111.332791.
27. **Collins PL, Mottet G.** 1993. Membrane orientation and oligomerization of the small hydrophobic protein of human respiratory syncytial virus. J. Gen. Virol. **74**(Part 7)**:**1445–1450.
28. **Kochva U, Leonov H, Arkin IT.** 2003. Modeling the structure of the respiratory syncytial virus small hydrophobic protein by silent-mutation analysis of global searching molecular dynamics. Protein Sci. **12:**2668–2674. http://dx.doi.org/10.1110/ps.03151103.
29. **Carter SD, Dent KC, Atkins E, Foster TL, Verow M, Gorny P, Harris M, Hiscox JA, Ranson NA, Griffin S, Barr JN.** 2010. Direct visualization of the small hydrophobic protein of human respiratory syncytial virus reveals the structural basis for membrane permeability. FEBS Lett. **584:**2786–2790. http://dx.doi.org/10.1016/j.febslet.2010.05.006.
30. **Madan V, Redondo N, Carrasco L.** 2010. Cell permeabilization by poliovirus 2B viroporin triggers bystander permeabilization in neighbouring cells through a mechanism involving gap junctions. Cell. Microbiol. **12:**1144–1157. http://dx.doi.org/10.1111/j.1462-5822.2010.01460.x.
31. **Suzuki T, Orba Y, Okada Y, Sunden Y, Kimura T, Tanaka S, Nagashima K, Hall WW, Sawa H.** 2010. The human polyoma JC virus agnoprotein acts as a viroporin. PLoS Pathog. **6:**e1000801. http://dx.doi.org/10.1371/journal.ppat.1000801.
32. **Schowalter RM, Smith SE, Dutch RE.** 2006. Characterization of human metapneumovirus F protein-promoted membrane fusion: critical roles for proteolytic processing and low pH. J. Virol. **80:**10931–10941. http://dx.doi.org/10.1128/JVI.01287-06.
33. **Smith EC, Culler MR, Hellman LM, Fried MG, Creamer TP, Dutch RE.** 2012. Beyond anchoring: the expanding role of the Hendra virus F protein transmembrane domain in protein folding, stability and function. J. Virol. **86:**3003–3013. http://dx.doi.org/10.1128/JVI.05762-11.
34. **Chang A, Hackett BA, Winter CC, Buchholz UJ, Dutch RE.** 2012. Potential electrostatic interactions in multiple regions affect human metapneumovirus F-mediated membrane fusion. J. Virol. **86:**9843–9853. http://dx.doi.org/10.1128/JVI.00639-12.
35. **Paterson RG, Lamb RA.** 1993. The molecular biology of influenza viruses and paramyxoviruses, p 35–73. *In* Davidson A, Elliott RM (ed), Molecular virology: a practical approach. IRL Oxford University Press, Oxford, United Kingdom.
36. **Burgess NK, Stanley AM, Fleming KG.** 2008. Determination of membrane protein molecular weights and association equilibrium constants using sedimentation equilibrium and sedimentation velocity. Methods Cell Biol. **84:**181–211. http://dx.doi.org/10.1016/S0091-679X(07)84007-6.
37. **Popa A, Carter JR, Smith SE, Hellman L, Fried MG, Dutch RE.** 2012. Residues in the Hendra virus fusion protein transmembrane domain are critical for endocytic recycling. J. Virol. **86:**3014–3026. http://dx.doi.org/10.1128/JVI.05826-11.
38. **Cole JL.** 2004. Analysis of heterogeneous interactions. Methods Enzymol. **384:**212–232. http://dx.doi.org/10.1016/S0076-6879(04)84013-8.
39. **Buchholz UJ, Finke S, Conzelmann KK.** 1999. Generation of bovine respiratory syncytial virus (BRSV) from cDNA: BRSV NS2 is not essential for virus replication in tissue culture, and the human RSV leader region acts as a functional BRSV genome promoter. J. Virol. **73:**251–259.
40. **Sabo Y, Ehrlich M, Bacharach E.** 2011. The conserved YAGL motif in human metapneumovirus is required for higher-order cellular assemblies of the matrix protein and for virion production. J. Virol. **85:**6594–6609. http://dx.doi.org/10.1128/JVI.02694-10.
41. **Niwa H, Yamamura K, Miyazaki J.** 1991. Efficient selection for high-expression transfectants by a novel eukaryotic vector. Gene **108:**193–200. http://dx.doi.org/10.1016/0378-1119(91)90434-D.
42. **Carter JR, Pager CT, Fowler SD, Dutch RE.** 2005. Role of *N*-linked glycosylation of the Hendra virus fusion protein. J. Virol. **79:**7922–7925. http://dx.doi.org/10.1128/JVI.79.12.7922-7925.2005.
43. **Fleming KG, Ackerman AL, Engelman DM.** 1997. The effect of point mutations on the free energy of transmembrane alpha-helix dimerization. J. Mol. Biol. **272:**266–275. http://dx.doi.org/10.1006/jmbi.1997.1236.
44. **Gatti PJ, Choi B, Haislip AM, Fermin CD, Garry RF.** 1998. Inhibition of HIV type 1 production by hygromycin B. AIDS Res. Hum. Retroviruses **14:**885–892. http://dx.doi.org/10.1089/aid.1998.14.885.
45. **Han Z, Licata JM, Paragas J, Harty RN.** 2007. Permeabilization of the plasma membrane by Ebola virus GP2. Virus Genes **34:**273–281. http://dx.doi.org/10.1007/s11262-006-0009-4.
46. **Rixon HW, Brown G, Aitken J, McDonald T, Graham S, Sugrue RJ.** 2004. The small hydrophobic (SH) protein accumulates within lipid-raft structures of the Golgi complex during respiratory syncytial virus infection. J. Gen. Virol. **85:**1153–1165. http://dx.doi.org/10.1099/vir.0.19769-0.
47. **Triantafilou K, Kar S, Vakakis E, Kotecha S, Triantafilou M.** 2013. Human respiratory syncytial virus viroporin SH: a viral recognition pathway used by the host to signal inflammasome activation. Thorax **68:**66–75. http://dx.doi.org/10.1136/thoraxjnl-2012-202182.
48. **Biacchesi S, Murphy BR, Collins PL, Buchholz UJ.** 2007. Frequent frameshift and point mutations in the SH gene of human metapneumovirus passaged *in vitro*. J. Virol. **81:**6057–6067. http://dx.doi.org/10.1128/JVI.00128-07.
49. **Lamb RA, Zebedee SL, Richardson CD.** 1985. Influenza virus M2 protein is an integral membrane protein expressed on the infected-cell surface. Cell **40:**627–633. http://dx.doi.org/10.1016/0092-8674(85)90211-9.
50. **Zebedee SL, Richardson CD, Lamb RA.** 1985. Characterization of the influenza virus M2 integral membrane protein and expression at the infected-cell surface from cloned cDNA. J. Virol. **56:**502–511.